

- Copyright permission to reproduce figures and/or text from this article

[View the Full Text HTML](#)



Crystal Structures of Salinosporamide A (NPI-0052) and B (NPI-0047) in Complex with the 20S Proteasome Reveal Important Consequences of β -Lactone Ring Opening and a Mechanism for Irreversible Binding

Michael Groll,^{*,†} Robert Huber,[‡] and Barbara C. M. Potts^{*,§}

Contribution from the Ludwig-Maximilians-University of Munich, Butenandtstr. 5, Building B, 81377 Munich, Germany, Max Planck Institute for Biochemistry, D-82152 Martinsried, Germany, and Nereus Pharmaceuticals, Inc., 10480 Wateridge Circle, San Diego, California 92121

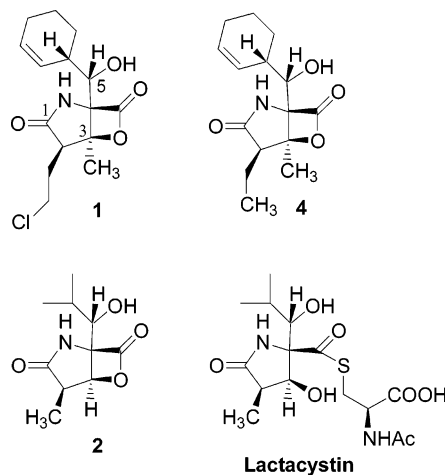
Received December 7, 2005; E-mail: Michael.Groll@med.uni-muenchen.de; bpotts@nereuspharm.com

Abstract: The crystal structures of the yeast 20S proteasome core particle (CP) in complex with Salinosporamides A (NPI-0052; **1**) and B (**4**) were solved at $<3 \text{ \AA}$ resolution. Each ligand is covalently bound to Thr1O γ via an ester linkage to the carbonyl derived from the β -lactone ring of the inhibitor. In the case of **1**, nucleophilic addition to the β -lactone ring is followed by addition of C-3O to the chloroethyl group, giving rise to a cyclic ether. The crystal structures were compared to that of the omuralide/CP structure solved previously, and the collective data provide new insights into the mechanism of inhibition and irreversible binding of **1**. Upon opening of the β -lactone ring, C-3O assumes the position occupied by a water molecule in the unligated enzyme and hinders deacylation of the enzyme–ligand complex. Furthermore, the resulting protonation state of Thr1NH₂ deactivates the catalytic N-terminus.

1. Introduction

Salinosporamide A (NPI-0052; **1**), a small molecule secondary metabolite of the marine actinomycete *Salinispora tropica*,^{1,2} is a highly potent and selective inhibitor of the 20S proteasome that is currently in development for the treatment of cancer.³ Although structurally related to omuralide (**2**),⁴ a β -lactone derived from the natural product lactacystin,⁵ salinosporamide A (**1**) contains several unique substituents, including a cyclohexene ring in place of the isopropyl group at C-5 and a chloroethyl group in place of methyl at C-2 (Chart 1), which collectively enhance its potency both in vitro and in vivo.^{1,6} We have recently shown that analogues with leaving groups such as bromine or iodine in place of chlorine are equipotent with **1** across a variety of biological assays. We also reported that cleavage of the β -lactone ring results in intramolecular nucleophilic addition to the chloroethyl group and concomitant formation of a tetrahydrofuran ring (**3**; Scheme 1). Together, these findings led us to propose a mechanistic role for the chloroethyl substituent.⁶

Chart 1. Structures of Salinosporamides A (**1**) and B (**4**), and Omuralide (**2**), Derived from Lactacystin



Since FDA approval of Velcade for the treatment of multiple myeloma in 2003, the 20S proteasome has represented a validated target for the treatment of cancer.⁷ This multicatalytic proteolytic complex plays a critical role in intracellular processes such as cell cycle regulation and cytokine-stimulated signal transduction.⁸ Current understanding of proteasomal structural biology has benefited from previous detailed studies, which have

[†] Ludwig-Maximilians-University of Munich.

[‡] Max-Planck Institute for Biochemistry.

[§] Nereus Pharmaceuticals, Inc.

(1) Feling, R. H.; Buchanan, G. O.; Mincer, T. J.; Kauffman, C. A.; Jensen, P. R.; Fenical, W. F. *Angew. Chem., Int. Ed.* **2003**, *42*, 355.

(2) Maldonado, L. A.; Fenical, W.; Jensen, P. R.; Kauffman, C. A.; Mincer, T. J.; Ward, A. C.; Bull, A. T.; Goodfellow, M. *Int. J. Syst. Evol. Microbiol.* **2005**, *55*, 1759.

(3) Chauhan, D. et al. *Cancer Cell*, **2005**, *8*, 407.

(4) Corey, E. J.; Li, W. Z. *Chem. Pharm. Bull.* **1999**, *47*, 1.

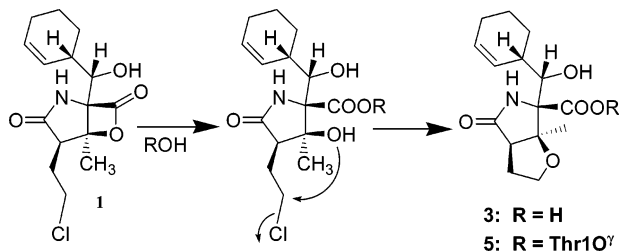
(5) Omura, S.; Matsuzaki, K.; Fujimoto, T.; Kosuge, K.; Furuya, T.; Fujita, S.; Nakagawa, A. *J. Antibiotics* **1991**, *44*, 117.

(6) Macherla, V. R. et al. *J. Med. Chem.* **2005**, *48*, 3684.

(7) Bross, P. F. et al. *Clin. Cancer Res.* **2004**, *10*, 3954.

(8) Adams, J. *Proteasome Inhibitors in Cancer Therapy*; Humana Press: Totowa, NJ, 2004.

Scheme 1. Mechanism of Hydrolysis and Further Rearrangement of **1** in Aqueous Solution (R = H) and Analogous Reaction Sequence that Occurs in the Binding Pocket of the Proteasome CP to Form **5** (R = Thr1O γ)⁶



revealed 28 subunits forming four stacked rings.^{9,10} The two central rings each contain three subunits ($\beta 5$, $\beta 2$, and $\beta 1$) that catalyze substrate hydrolysis with the following specificities: chymotrypsin-like (CT-L), trypsin-like (T-L), and PGPH or caspase-like (CA-L) activity, respectively. These six catalytic subunits each possess an N-terminal nucleophilic threonine residue and are thus members of the N-terminal nucleophile hydrolase family of enzymes.¹¹ Proteasome CPs have substrate binding channels of about eight amino acids in length, denoted S1–S8. The S1 binding pocket is involved in key enzyme–substrate interactions during hydrolysis of peptide bonds and confers specificity to each of the catalytic subunits. Understanding of the molecular mechanism of this catalytic machinery has evolved from detailed studies of the 20S proteasome core particle (CP) in complex with a wide variety of inhibitors, including **2** (derived from its naturally occurring precursor lactacystin) and epoxomicin, two natural product proteasome inhibitors that form covalent adducts with the catalytic threonine residue.^{9,12} Given the structural similarities between **1** and **2**, it is reasonable to expect that the β -lactone ring of **1** reacts similarly to **2**, forming an ester linkage between the Thr1OH γ and the β -lactone carbonyl. However, the enhanced potency of **1** requires further explanation. We therefore determined the structure of **1** in complex with the yeast 20S proteasome, presented herein at 2.8 Å resolution. For comparative analysis, we also evaluated an analogous complex comprising the recently described deschloro analogue **4**.^{6,13} and the proteasome CP at 2.9 Å resolution.

2. Results and Discussion

Salinosporamide A (**1**) was cocrystallized with the yeast 20S proteasome by soaking a single proteasome crystal with **1** for 60 min at a final concentration of 5 mM; a complex with compound **4** was prepared similarly. Crystallographic refinement started from the coordinates of the yeast 20S proteasome⁹ followed by anisotropic overall temperature factor correction and positional refinement using CNS¹⁴ and cyclic 2-fold symmetry averaging using MAIN.¹⁵ Electron density maps

calculated with phases after averaging allowed a detailed interpretation of compounds **1** and **4** (Figure 1). Both inhibitors are covalently bound to the N-terminal threonine residues of all six catalytic subunits. These findings are in contrast to results achieved with omuralide (**2**), which was found to occupy only the two $\beta 5$ subunits.⁹

The experimental electron density map of **1** in complex with subunit $\beta 5$ is shown in Figure 1a. As anticipated based on previous studies with **2**,⁹ the carbonyl carbon atom derived from the β -lactone ring is covalently bound to the catalytic N-terminal Thr1O γ . Uniquely, however, C3–O forms a cyclic tetrahydrofuran (THF) ring with the C-2 side chain (**5**). These findings, together with the knowledge that **3** (which contains a free carboxylic acid and preformed THF ring) does not inhibit the proteasome (IC₅₀ > 20 mM),⁶ support a two-step mechanism in which addition of Thr1OH γ to the β -lactone carbonyl is followed by nucleophilic addition of C-3O to the chloroethyl group, giving rise to cyclic ether **5**. The reactivity at the enzyme active site is analogous to the pathway predicted from reactions in aqueous solution (Scheme 1).⁶

To directly compare salinosporamides A (**1**) and B (**4**) with omuralide (**2**) in their bound forms, subunit $\beta 5$ of the various CP/inhibitor complexes were structurally superimposed (rms values for all atoms of CP/**1** versus CP/**4** and for CP/**1** versus CP/**2** are 0.36 Å and 0.49 Å, respectively) (Figure 1d). Comparison of all three crystal structures reveals a unique binding mechanism for this class of inhibitors. Key interactions (Figure 2) comprise the covalent bond with Thr1O γ and hydrophobic interactions between the C-5 substituent and the S1 binding pocket, as well as strong implications of an important role for C-3O in the inhibition and an irreversible binding mechanism.

With respect to the ligands, **1** is structurally distinct from **2** and **4** by virtue of its leaving group ability. The unreactive methyl and ethyl C-2 substituents of **2** and **4**, respectively, circumvent formation of the THF ring. The positions of the methylene carbons of the bound form of **1** are fixed by the THF ring, while the corresponding carbon atoms of **4** are unrestricted and assume a different orientation. The C-2 substituents project into empty space. Thus, there is sufficient space to accommodate a methyl group, an ethyl group, or a THF ring, and perhaps larger side chains, some examples of which have been reported previously.^{6,19} However, because the S2 pocket is an open cavity, there are no apparent contacts between P2 (the C-2 substituent) and the protein. It is therefore difficult to predict the optimal structure for the side chain based on the X-ray crystal structure of the complex.

The C-3 methyl group of **1** and **4** points toward a small pocket and weakly interacts with the protein. Clearly, both a hydrogen (**2**) and a methyl group are accommodated within this pocket, with the latter having distances of ≤ 3.6 Å to neighboring residues Arg190, Thr21N, Thr21O γ , and Tyr168O. Previously reported results for a fermentation analogue containing an ethyl group at this position demonstrate that this compound does not inhibit the proteasome.⁶ This is consistent with the structural

(9) Groll, M.; Ditzel, L.; Löwe, J.; Stock, D.; Bochtler, M.; Bartunik, H. D.; Huber, R. *Nature* **1997**, *386*, 463.

(10) Löwe, J.; Stock, D.; Jap, B.; Zwickl, P.; Baumeister, W.; Huber, R. *Science* **1995**, *268*, 533.

(11) Groll, M.; Bochtler, M.; Brandstetter, H.; Clausen, T.; Huber, R. *Chem-BioChem* **2005**, *6*, 222.

(12) Groll, M.; Kim, K. B.; Kairies, N.; Huber, R.; Crews, C. M. *J. Am. Chem. Soc.* **2000**, *122*, 1237.

(13) Williams, P. G.; Buchanan, G. O.; Feling, R. H.; Kauffman, C. A.; Jensen, P. R.; Fenical, W. *J. Org. Chem.* **2005**, *70*, 6196.

(14) Brünger, A. et al. *Acta Crystallogr., Sect. D* **1998**, *1*, 905.

(15) Turk, D. 1992. Improvement of a program for molecular graphics and manipulation of electron densities and its application for protein structure determination. Thesis, Technische Universität München.

(16) Merritt, E. A.; Murphy, M. E. *Acta Crystallogr., Sect. D* **1994**, *1*, 869.

(17) Esnouf, R. M. *J. Mol. Graphics Modell.* **1997**, *15*, 132, 112.

(18) Nicholls, A.; Sharp, K.; Honig, B. *Proteins: Struct., Funct., Genet.* **1991**, *11*, 281ff.

(19) Stadler, M. et al. International Application Published Under the Patent Cooperation Treaty, WO 2004/071382 A2.

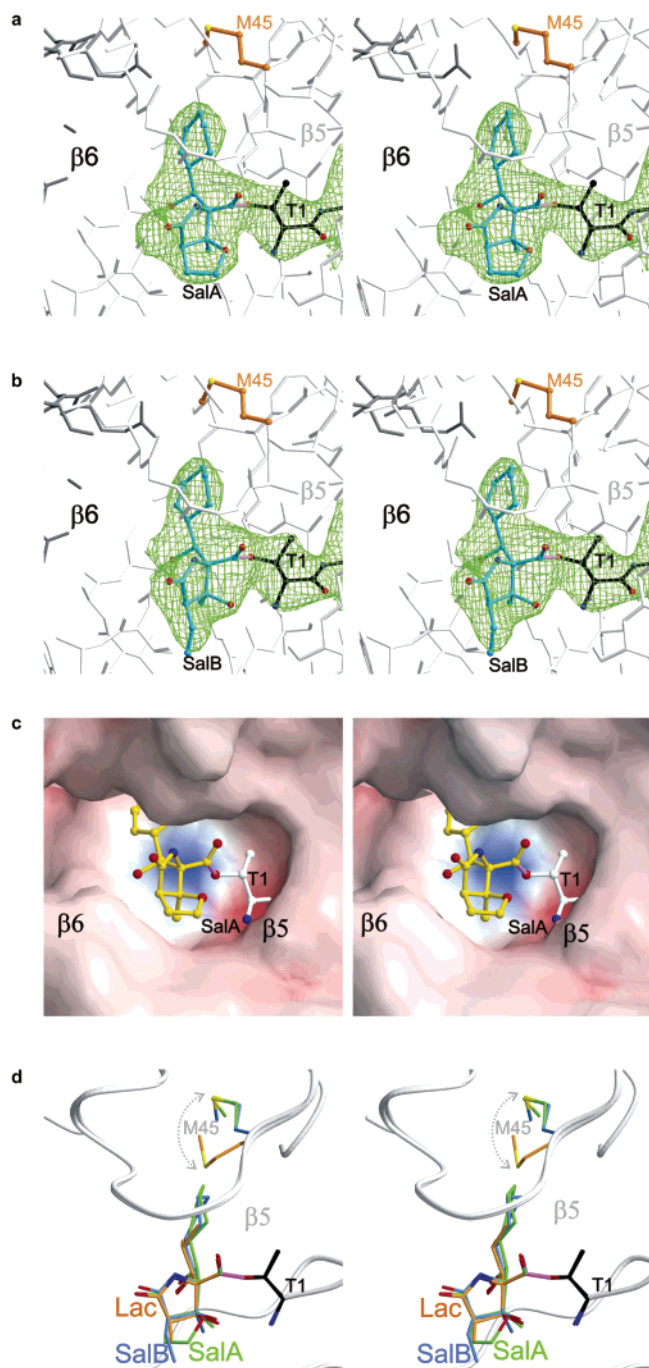


Figure 1. Stereo representation of the CT-L active site of the yeast 20S proteasome (subunit $\beta 5$, white; subunit $\beta 6$, gray) in complex with (a) Salinosporamide A and (b) Salinosporamide B (colored in cyan). Covalent linkage of inhibitors with Thr1 is drawn in magenta. Met45 (orange) of subunit $\beta 5$ specifically interacts with the P1-side chain of both ligands. Electron density maps (green) are contoured from 1σ in similar orientations around Thr1 (black) with $2F_o - F_c$ coefficients after 2-fold averaging. Apart from the bound inhibitor molecules, structural changes were only noted in the specificity pockets. Temperature factor refinement indicates full occupancies of all inhibitor binding sites. Inhibitors have been omitted for phasing.^{16,17} (c) Surface model of **1** bound to subunit $\beta 5$. Thr1 (white) is covalently linked to the inhibitor. Colors indicate positive and negative electrostatic potentials contoured from $15kT/e$ (intense blue) to $-15kT/e$ (intense red).¹⁸ (d) Superposition of the coordinates of **1** (green) and **4** (blue) with **2** (orange). The protein is represented as coils, whereas ligands, Thr1 (black), and Met45 (color coded according to the various inhibitors) are shown as ball-and-stick representation. Note the similar binding mode for all three inhibitors within the active site of the proteasome but different architecture of the S1 pocket due to the relative position of Met45 in the presence of **1** and **4** versus **2**.

data reported herein, which indicate that the ethyl group is too large and would result in steric interactions that do not accommodate binding.

With respect to C-5OH, we have previously shown that epimerization or oxidation to the ketone results in analogues that do not show any proteasomal inhibition.⁶ The crystallographic data presented herein indicate that both forms would introduce unfavorable steric interactions with the protein (specifically, epi-C-5-OH would clash with Lys33, and C-5=O would clash with Arg19CO). In contrast, the reduced form of **1** containing a methylene group at C-5 is a potent proteasome inhibitor, albeit 20-fold weaker than **1** in terms of CT-L inhibition.²⁰ This is consistent with findings for the C-5H₂ analogue of **2**, which was over 10-fold less potent than omuralide.⁴ The diminished potency of the C5-H₂ analogue suggests an important role for C5-OH in **1**, **2**, and **4**. In all three crystal structures, hydrogen bonds are evident between C-5-OH and Thr21NH. In terms of the γ -lactam ring, the amide NH binds to Gly47O (2.9 Å).

The most critical observations deduced from the crystal structures of the ligand/CP complexes reported herein relate to the consequences of β -lactone ring opening and our proposal for the mechanism for irreversible binding of Salinosporamide A. It is therefore important to discuss the catalytic mechanism in some detail (Scheme 2). The collective data from this and previous studies^{10,21} support a mechanism whereby nucleophilic addition of Thr1O γ to the substrate peptide bond carbonyl is catalyzed by a deprotonated N-terminus, which is positioned to accept the Thr1O γ proton, either directly or via a water molecule. Peptide bond cleavage likely occurs through a tetrahedral intermediate in which the oxyanion is stabilized by Gly47N. Finally, the deprotonated N-terminus catalyzes the addition of a nucleophilic water molecule to the Thr1O γ -CO acyl ester intermediate, cleaving the ester bond (Scheme 2a). A structurally prearranged water molecule termed NUK was previously implicated in shuttling a proton between Thr1O γ and the N-terminus during this process.^{10,22} Our current evaluation indicates that unligated forms of the proteasome CP retain a series of well-defined water molecules²³ in close proximity to Gly47N, in the vicinity of Thr1O γ , and adjacent to Thr1N. This suggests that there is not just a single water molecule involved in proton shuttling but a defined number of water molecules comprising a small hydrogen bonding network that are activated by the formation of hydrogen bonds to the protein. Interestingly, the structures of the CP in complex with **1**, **2**, and **4** indicate that the water molecules are generally disordered. Significantly, after the lactone ring of **2** or **4** is cleaved, C-3OH occupies the position formerly assumed by a well-defined water molecule in the unligated form. The γ -lactam ring prevents free rotation about the C-3/C-4 bond, helping to maintain C-3O in this position. In **1**, C-3O is similarly situated and further fixed in position by the THF ring. As the preferred trajectory of nucleophilic addition^{24,25} is along the path approximately

(20) Reed, K. A.; Manam, R. R.; Mitchell, S. S.; Chao, T.; Teisan, S.; Lam, K. S.; Potts, B. C. M., in preparation.

(21) Groll, M.; Heinemeyer, W.; Jäger, S.; Ullrich, T.; Bochtler, M.; Wolf, D. H.; Huber, R. *Proc. Natl. Acad. Sci. U.S.A.* **1999**, *96*, 10976.

(22) Ditzel, L.; Huber, R.; Mann, K.; Heinemeyer, W.; Wolf, D. H.; Groll, M. *J. Mol. Biol.* **1998**, *279*, 1187.

(23) The electron density in this region is rather large, indicating that there are more water molecules (about 3 to 4). It also has high I/Sigmal values, indicating that these locations are specific.

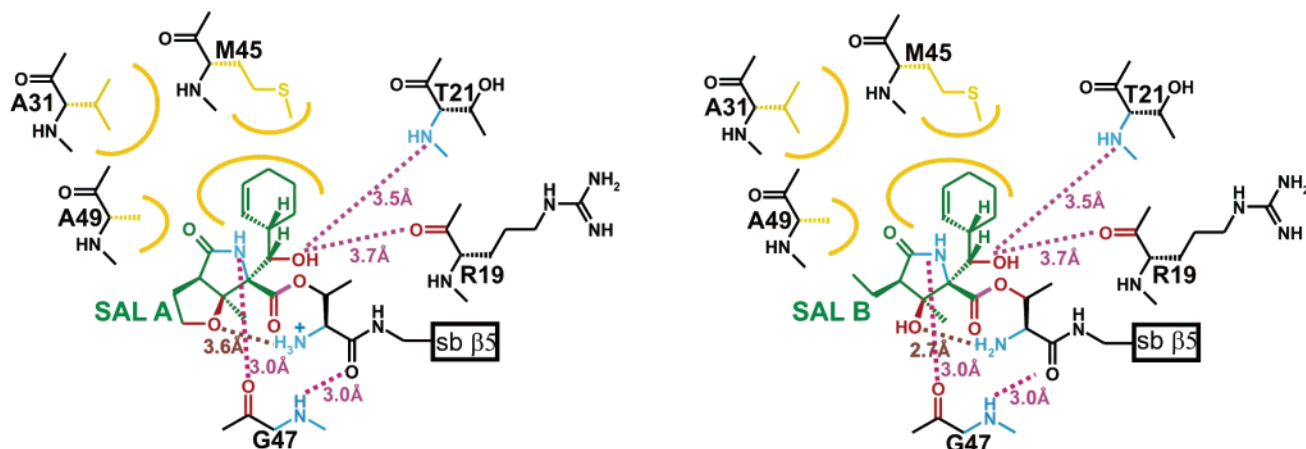


Figure 2. Key contacts between amino acids of the ligand binding site of the 20S proteasome core particle and **1** (left) and **4** (right). Atoms within hydrogen bonding distance are shown in purple. Hydrophobic interactions between P1 (cyclohexene) and S1 are shown in yellow.

perpendicular to the plane of the ester group, the two possible faces of attack on Thr1O γ –CO by water are blocked by C3–O on one side of the plane (*re*) and by the P1 side chain (C-5 substituent) and protein residues on the other side of the plane (*si*). By blocking access to nucleophilic water, C-3O would be expected to interfere with deacylation of Thr1O γ . However, based on published data for a synthetic analogue of **2**, the covalent ester bond between the proteasome and inhibitors **2** and **4** should be slowly reversible.²⁶ The reversibility could be attributed to aqueous hydrolysis, suggesting that water may ultimately penetrate this “C-3O barrier.” Alternatively, it may result from reformation of the β -lactone ring. The energetics of both pathways is not defined,²⁷ but the N-terminus could catalyze either of these reactions by deprotonating C-3OH, which is well positioned to deacylate ThrO γ , or a water molecule. In the case of **1**, C-3O is engaged in the THF ring, circumventing any possibility of regenerating the β -lactone. Finally, based on the mechanism outlined above for substrate hydrolysis, it is reasonable to hypothesize that upon opening the β -lactone ring of **2** and **4**, the Thr1O γ proton is transferred to C-3O (instead of water). As C-3OH is within hydrogen bonding distance of the N-terminus (2.7 Å), a partial positive charge is effectively placed on Thr1NH $_2$. In the case of **1**, upon opening of the β -lactone ring, the N-terminus is positioned to abstract the proton from C-3OH and catalyze formation of the cyclic ether. In the final adduct, C-3O is tied up within the THF ring (3.6 Å from the N-terminus) and therefore not protonated, thus, the proximal N-terminus fully absorbs the proton and bears the full positive charge. While the partially

protonated N-terminus (in the presence of **2** and **4**) might retain some potential to catalyze deacylation (*vide supra*), the fully protonated N-terminus (in the presence of **1**) should be completely inactivated, rendering the proteasome irreversibly inhibited.²⁸

In addition to the unique protonation states of the N-terminus resulting from interactions with **1** versus **4**, the improved potency of **1** may be further attributed to the C-2 substituent as follows. While both molecules contain flexible C-2 side chains that putatively generate entropic loss upon binding, the chloroethyl “trigger” of **1** may provide an enthalpically and entropically favorable binding mechanism associated with the release of HCl. Thus, the chlorine may enhance proteasome inhibition through more favorable binding energy while providing the parallel benefit of increased potential for membrane permeability.²⁹ It is interesting to note that omuralide (**2**) is found in nature in the form of its precursor thioester lactacystin, which contains a free C3–OH group (Chart 1). In contrast, thioesters of **1** have not been reported; such forms of the molecule would give rise to chlorine elimination, prematurely releasing this trigger.

A final point of discussion relates to the impact of increasing the size of the P1 site (*i.e.*, the C-5 substituent) from an isopropyl group (**2**) to a cyclohexenyl ring (**1** and **4**). These substituents interact with Met45 of the β 5 S1 binding pocket, which is involved in key enzyme–substrate interactions during hydrolysis of peptide bonds containing hydrophobic amino acids (*i.e.*, CT-L activity).³⁰ To accommodate the larger cyclohexenyl ring of **1** and **4**, Met45 shifts 2.7 Å from its position in the **2**/ β 5 structure (Figure 1d). Although the flexibility of side chains in proteins makes it difficult to predict optimal substitution at this site, we note that **1** and **4** are more potent inhibitors of the CT-L activity of rabbit 20S proteasome³¹ than **2** (IC₅₀ 2.6 nM, 27 nM, and 57 nM, respectively).⁶ Our structural data indicate that additional hydrophobic interactions are found between atoms of the

(24) Huber, R.; Bode, W. *Acc. Chem. Res.* **1978**, *11*, 114–122.

(25) Bürgi, H. B.; Dunitz, J. D.; Shefter, E. *J. Am. Chem. Soc.* **1973**, *95*, 5065.

(26) While **2** has been reported to bind irreversibly to the proteasome (Fenteany, G.; Standaert, R. F.; Lane, W. S.; Choi, S.; Corey, E. J.; Schreiber, S. L. *Science* **1995**, *268*, 726), data on a closely related synthetic analogue PS-519 indicate that the binding, while covalent, is reversible, with full recovery of blood 20S proteasome activity to basal levels within 24 h post administration (Shah, I. M.; Lees, K. R.; Pien, C. P.; Elliot, P. J. *J. Clin. Pharmacol.* **2002**, *54*, 269). In contrast, blood 20S proteasome activity was only partially recovered after 7 days in mice treated with **1**;³ this recovery may be attributed to red blood cell turnover.

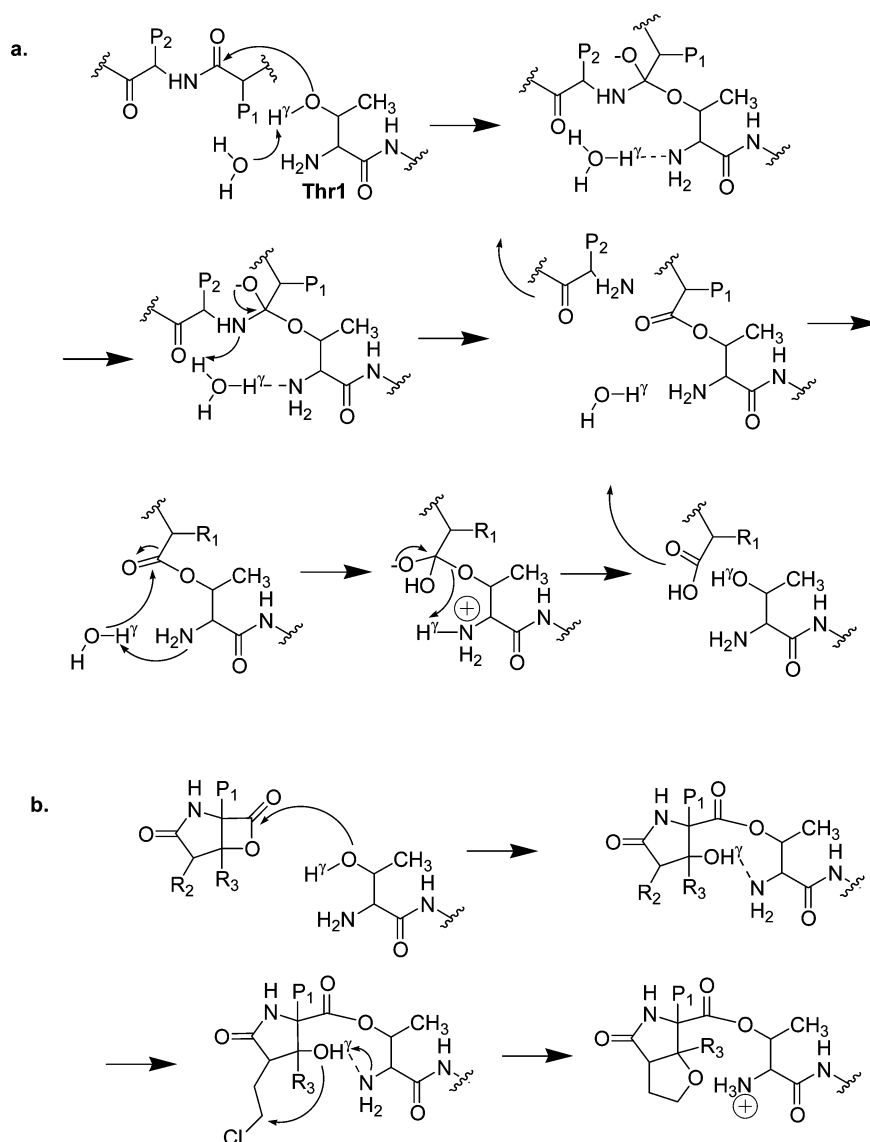
(27) In studies of β -lactone inhibitors of serine proteases, it has been suggested that the initial acyl-enzyme intermediate formation may be largely driven by relief of the high strain energy of the β -lactone ring and that the putative tetrahedral intermediate may not be stabilized by an oxyanion hole, *i.e.*, may not be enzymatically driven (Kim, D.; Park, J.; Chung, S. J.; Park, J. D.; Park, N.; Han, J. H. *Bioorg. Med. Chem.* **2002**, *10*, 2553). Reformation of the β -lactone ring would require overcoming a high energy barrier. Although this might be enzymatically catalyzed, once reformed, it would be expected to once again react quickly with the ThrO γ nucleophile.

(28) A similar mechanism has been proposed for the inhibition of serine proteases. See Li, Z.; Bulychev, A.; Kotra, L. P.; Massova, I.; Mobashery, S. *J. Am. Chem. Soc.* **1998**, *120*, 13003.

(29) **1** is 2–3 log units more potent in whole cell assays than **4**,⁶ which may be partially attributed to enhanced membrane permeability.

(30) Because **2** does not bind to β 1 and β 2 in the crystal structure, our discussions are focused on β 5.

(31) A structural superposition of a yeast wild-type core particle and bovine liver core particle shows a near perfect fit, validating structural comparisons of yeast and mammalian proteasome structures.

Scheme 2^a

^a (a) Hydrolysis of the peptide substrate as catalyzed by the active site amino acids. The unprotonated N-terminus catalyzes the abstraction of the Thr1O γ proton and nucleophilic addition of Thr1O γ to the substrate carbonyl, which results in hydrolysis of the peptide bond via a tetrahedral intermediate. Deacylation of Thr1O γ is catalyzed by an unprotonated N-terminus. (b) Thr1O γ is similarly acylated by the inhibitor as has been described for the peptide substrate and might similarly occur through a tetrahedral intermediate (not shown).²⁷ Cleavage of the acyl-ester intermediate by the nucleophilic water molecule is challenged by the special arrangement of C-3O of the inhibitor at the active site. In the case of **2** and **4**, the N-terminus is positioned for hydrogen bonding with the inhibitor C-3OH. In the case of **1**, chlorine is eliminated and the N-terminus is fully protonated.

cyclohexene ring and residues of the S1-pocket for subunit $\beta 5$, thus corresponding to the enhanced potency of **1** and **4** as compared to **2**. Nevertheless, the C-5 substituent presents a relatively limited surface for binding to the enzyme. In the context of proteasome inhibitors, which typically bind to several substrate binding pockets of the proteasome (S1, S3, and S4), **1**, **2**, and **4** are comparatively short, yet they still show excellent inhibitory activity, suggesting that hydrophobic interactions between the C-5 substituent and the S1 site allow sufficient residence time in the binding pocket for covalent addition by the N-terminal threonine residue to occur.

This unique class of ligands may represent the ultimate in efficiency among proteasome inhibitors.³² The C-5 substituent provides sufficient interaction with the S1 binding site to allow the highly reactive β -lactone ring to form a covalent adduct

with Thr1O γ , resulting in the spontaneous unveiling of C-3O, which is fixed in position by the γ -lactam ring and ultimately protects the inhibitor from hydrolysis and elimination. In the case of the salinosporamides, the cyclohexenyl ring offers additional hydrophobic interactions at the S1 binding site that are not available to omuralide. Furthermore, the unique chloroethyl trigger of **1** is expected to provide favorable enthalpic and entropic binding energy, with release of this trigger catalyzed by the N-terminus. In its final cyclic ether form, Salinosporamide A is irreversibly bound by virtue of the "C-3O barrier" to penetration by water and a fully protonated and deactivated N-terminus that collectively prevent Thr1O γ from being deacylated. It is difficult to envision a more elegant design than that created by nature, which has provided for streamlined binding, reactivity, and irreversible inhibition in a densely yet minimally functionalized inhibitor.

(32) Groll, M.; Huber, R. *Biochim. Biophys. Acta* **2004**, *1695*, 33.

3. Experimental Section

Cocrystallization. Crystals of the 20S proteasome from *S. cerevisiae* were grown in hanging drops at 24 °C as already had been described⁹ and incubated for 60 min with the natural compound **1** or **4**. The protein concentration used for crystallization was 40 mg/mL in Tris-HCl (10 mM, pH 7.5) and EDTA (1 mM). The drops contained 3 μ L of protein and 2 μ L of the reservoir solution, containing 30 mM of magnesium acetate, 100 mM of morpholino-ethane-sulfonic acid (pH 7.2), and 10% of MPD.

The space group belongs to $P2_1$ with cell dimensions of about $a = 135$ Å, $b = 301$ Å, $c = 144$ Å, and $\beta = 113^\circ$ (see Supporting Information). Data to 2.8 Å for the CP/**1** and to 2.9 Å for the CP/**4** complex were collected using synchrotron radiation with $\lambda = 1.05$ Å on the BW6-beamline at DESY/ Hamburg/Germany. Crystals were soaked in a cryoprotecting buffer (30% MPD, 20 mM of magnesium acetate, 100 mM of morpholino-ethane-sulfonic acid pH 6.9) and frozen in a stream of liquid nitrogen gas at 90 K (Oxford Cryo Systems). X-ray intensities were evaluated by using the MOS-FILM program package (version 6.1), and data reduction was performed with CCP4.³³ The anisotropy of diffraction was corrected by an overall

(33) Otwinowski, Z.; Minor, W. Processing of X-ray Diffraction Data Collected in Oscillation Mode. In *Macromolecular Crystallography, Part A*; Carter, C. W., Jr., Sweet, R. M., Eds.; Methods in Enzymology, Volume 276; Academic Press: New York, 1997; pp 307–326.

anisotropic temperature factor by comparing observed and calculated structure amplitudes using the program CNS.¹⁴ Electron density was improved by averaging and back transforming the reflections 10 times over the 2-fold noncrystallographic symmetry axis using the program package MAIN.¹⁵ Conventional crystallographic rigid body, positional, and temperature factor refinements were carried out with CNS¹⁴ using the yeast 20S proteasome structure as a starting model.⁹ For model building the program MAIN was used. Modeling experiments were performed using the coordinates of yeast 20S proteasome with the program MAIN.¹⁵

Protein Data Bank Accession Codes. Coordinates have been deposited in the RCSB Protein Data Bank under the accession code 2FAK.

Acknowledgment. Dedicated to William Fenical on the occasion of his 65th Birthday. We are grateful to Gleb Bourenkov for his valuable help during crystal measurements at the Deutsche Elektronen Synchrotron facilities in Hamburg.

Supporting Information Available: Table of crystallographic data collection and refinement statistics. Complete refs 3, 6, 7, 14, and 19. This material is available free of charge via the Internet at <http://pubs.acs.org>.

JA058320B